Asymmetric C-13-C-13 polarization transfer under dipolar-assisted rotational resonance in magic-angle spinning NMR

AUTHOR(S):

Ohashi, R; Takegoshi, K

THE JOURNAL OF CHEMICAL PHYSICS **125**, 214503 (2006)

Asymmetric $^{13}C-^{13}C$ polarization transfer under dipolar-assisted rotational resonance in magic-angle spinning NMR

Ryutaro Ohashi and K. Takegoshi[a)]
Department of Chemistry, Graduate School of Science, Kyoto University, Kitashirakawaoiwake-cho, Sakyo-ku, Kyoto 606-8502, Japan

(Received 21 June 2006; accepted 25 September 2006; published online 4 December 2006)

A two-dimensional (2D) homonuclear exchange NMR spectrum in solids often shows an asymmetric cross-peak pattern, which disturbs a quantitative analysis of peak intensities. When magnetization is prepared using cross polarization (CP), the asymmetry can naively be ascribed to nonequilibrium initial magnetization. We show, however, that the CP effect cannot fully explain the observed mixing-time dependence of the peak intensities in 2D $^{13}C-^{13}C$ exchange spectra of [2,3-^{13}C] *l*-alanine (2,3-Ala) under $^{13}C-^{1}H$ dipolar-assisted rotational resonance (DARR) recoupling, which has recently been proposed for a broadband recoupling method under magic-angle spinning. We develop a theory to describe polarization transfer in a two-spin system under DARR recoupling. By taking into account the effects of the partial spectral overlap among ^{13}C signals, which is a unique feature of DARR recoupling, and $^{1}H-^{1}H$ flip-flop exchange, we can successfully explain the observed mixing-time dependence of the peak intensities of 2D $^{13}C-^{13}C$ DARR exchange spectra of 2,3-Ala. A simple initial-rate analysis is also examined.
 [DOI: 10.1063/1.2364503]

I. INTRODUCTION

Two-dimensional (2D) homonuclear exchange NMR is a useful tool for studying chemical exchange process.[1] Further, by monitoring polarization transfer among spins, we can assign signals and obtain geometrical information of a molecule.[1] For example, the 2D exchange experiment using polarization transfer among ^{1}H spins by nuclear Overhauser effect (NOE) has been applied to determine a structure of protein molecules in solution.[2] While in solids, $^{13}C-^{13}C$ polarization transfer was utilized to determine a structure of protein molecules, such as the α-spectrin SH3 domain,[3] where $^{13}C-^{13}C$ polarization transfer is realized with a so-called ^{1}H-driven method.[4] To facilitate $^{13}C-^{13}C$ polarization transfer in solids, several $^{13}C-^{13}C$ polarization transfer methods applicable under magic-angle spinning (MAS) have been proposed, to name a few examples, radio frequency-driven dipolar recoupling (RFDR),[5] double-quantum homonuclear rotary resonance (HORROR),[6] combined rotation with nutation (CROWN),[7] seven phase-shifted radiofrequency pulse cycles (C7),[8] and dipolar-assisted rotational resonance (DARR).[9,10] So far, DARR has been applied for signal assignment of protein molecules such as GB1 (Ref. 11) and ubiquitin.[12] For signal assignment, short polarization-transfer times (mixing time τ_m) of ~10 ms, during which magnetization exchange between most of directly bonding $^{13}C-^{13}C$ pairs can be observed, were used. To monitor polarization transfer for distant (~0.3 nm) $^{13}C-^{13}C$ pairs, a longer mixing time ($\tau_m \geqslant 100$ ms) was required as shown in the 2D exchange experiment using DARR recoupling for rhodopsin.[13] DARR with a longer mixing time has also been applied for structural analysis of selectively ^{13}C-labeled Alzheimer's β-amyloid fibrils.[14]

By examining several 2D $^{13}C-^{13}C$ exchange spectra in solids, we found that intensities of a pair of cross peaks are often unequal. For example, let us examine a 2D exchange spectrum [Fig. 1(a)] of fully ^{13}C-labeled N-acetyl-*l*-prolylglycil-*l*-phenylalanine using DARR recoupling with τ_m of 10 ms. Apparently, the cross peak corresponding to that observed at (F1,F2)=(38.6,138.9) ppm is missing. Further, the (F2, F1) cross peaks associated with (F1,F2)=(28.2,174.6) and (38.6,172.2) ppm are not appreciable. Figure 1(b) summarizes distribution of the ratio of the (F2, F1) cross-peak intensities to the corresponding (F1, F2) ones. In the 18 pairs of cross peaks observed, only two pairs are almost symmetric (the ratios are 0.9–1.1), and the remaining 16 pairs are asymmetric (the ratios are 0.3–0.9 or 1.1–1.3). This apparent asymmetry in the 2D exchange spectrum cannot be interpreted intuitively because the intensities of a pair should be equal when the mixing process retains microscopic reversibility and the initial magnetization is prepared nonselectively.[15] The asymmetry in cross-peak intensities is not quite obstructive to signal assignment, however, for determination of a molecular structure quantitative signal analysis is required. In this work, we developed a theory to explain the asymmetric cross-peak intensities in 2D exchange spectra and compared with experimental results for a two ^{13}C-spin system in [2,3-^{13}C] *l*-alanine (2,3-Ala). The observed apparent asymmetry in 2D exchange spectra using DARR recoupling was ascribed to the use of cross polarization (CP), the character-

a)Electronic mail: takeyan@kuchem.kyoto-u.ac.jp

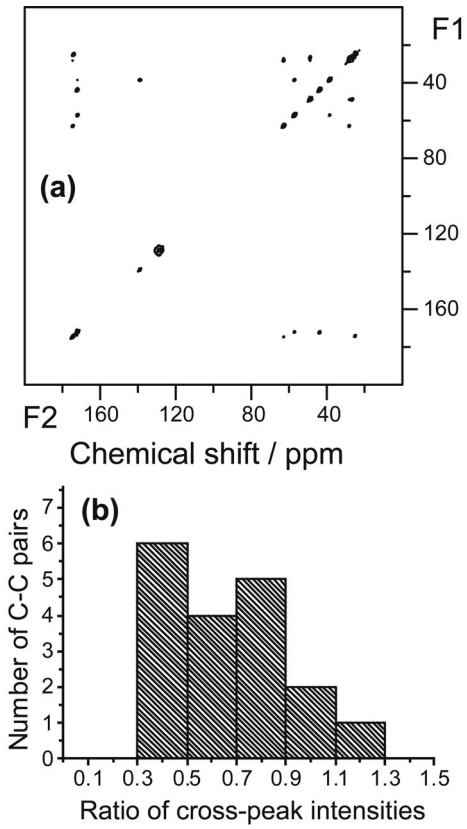

FIG. 1. (a) $^{13}C-^{13}C$ 2D exchange NMR spectrum of [U−^{13}C, ^{15}N]-labeled N-acetyl-*l*-prolylglycil-*l*-phenylalanine diluted 1:10 with unlabeled one. The spectrum was taken with DARR at $\tau_m = 10$ ms. (b) Histogram of the distribution of the ratios of cross-peak intensities of pair spins in the spectrum of Fig. 1(a).

istic feature of DARR recoupling, that is, orientation-dependent recoupling,[10] and the flip-flop transition of ^{1}H spins.

II. EXPERIMENTAL DETAILS

[2,3-^{13}C] *l*-alanine (2,3-Ala) was purchased from Cambridge isotope Laboratories, Inc, and used without purification. Fully ^{13}C- and ^{15}N-labeled N-acetyl-*l*-prolylglycil-*l*-phenylalanine (Pro-Gly-Phe) was synthesized using the Fmoc method, purified with a reverse phase HPLC, and finally freeze dried. To minimize intermolecular $^{13}C-^{13}C$ coupling, [U−^{13}C, ^{15}N]-labeled Pro-Gly-Phe was diluted 1:10 with unlabeled one. White crystalline needles[16] were obtained from hot hexane and ethanol solution, which were ground for solid-state NMR.

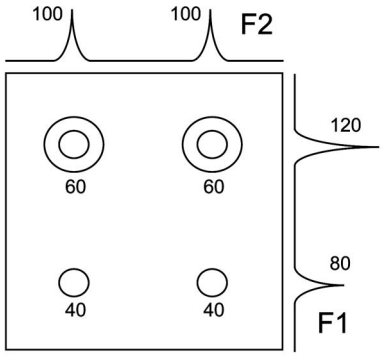

FIG. 2. Schematic illustration of a 2D contour spectrum of two exchanging magnetizations starting from nonequilibrium initial magnetization with a ratio of 120:80. The projection spectrum in the first domain (F1) thus shows two peaks with the intensity ratio of 120:80, while that in F2 assumes thermal equilibrium (100:100). Each figure associated with the peaks denotes its relative intensity.

The NMR experiments were carried out by using a Chemagnetics Infinity spectrometer operating at 100 MHz for ^{13}C and at 400 MHz for ^{1}H with a Chemagnetics MAS probe for a 3.2 mm rotor. All experiments were done at the spinning frequency (ν_R) of 20 kHz and at room temperature. DARR recoupling was done by applying ^{1}H cw irradiation with the ^{1}H rf intensity equal to the spinning frequency.[9,10] two-pulse phase modulation (TPPM) decoupling[17] was used with the phase-modulation angle of ±10.5° and the rf intensity of 120 kHz. For CP enhancement, the ^{1}H rf intensity was 50 kHz and ^{13}C rf intensity was varied from 66 to 74 kHz stepwise.

III. RESULT AND DISCUSSION

A. Effects of CP

In 2D exchange NMR experiments with CP, asymmetric cross-peak intensities can simply be ascribed to nonuniform CP signal enhancement. Suppose we observe a 2D exchange spectrum of two spins, *A* and *B*, with the initial magnetization being prepared by CP with an unequal intensity ratio, say, 120:80. After a mixing time long enough to achieve internal equilibrium among *A* and *B*, the intensity ratio would become 100:100 if the spin-lattice relaxation can be ignored. Then the resulting 2D spectrum may be schematically represented in Fig. 2, showing an asymmetric 2D spectrum. For the experiment with CP, it is therefore easy to explain the asymmetry in the extreme case of a long mixing time.

In the following, we examine the mixing-time dependence of peak intensities on the basis of a theory developed for 2D exchange NMR using three $\pi/2$ pulses.[15] For ^{13}C experiments in solids, CP enhancement is used [Fig. 3(a)] instead of the first $\pi/2$ pulse in the original sequence. Even with this difference, the 2D exchange NMR spectrum $S(\omega_1, \tau_m, \omega_2)$ can formally be written as[15]

$$S^+(\omega_1,\tau_m,\omega_2) = -\sum_k \sum_l \frac{1}{i(\Omega_k-\omega_2)}[\exp(\mathbf{L}\tau_m)]_{k,l} \times \mathrm{Re}\left[\frac{1}{j(\Omega_l-\omega_1)}\right] M_{0,l}. \quad (1)$$

The symbols in Eq. (1) carry their original meanings given in Ref. 15. We assume that the polarization-transfer process between the methyl and the methine carbons in 2,3-Ala is simply expressed by using the following exchange matrix

$$\mathbf{L} = \begin{pmatrix} -R_{AA} & K \\ K & -R_{BB} \end{pmatrix}, \quad (2)$$

with

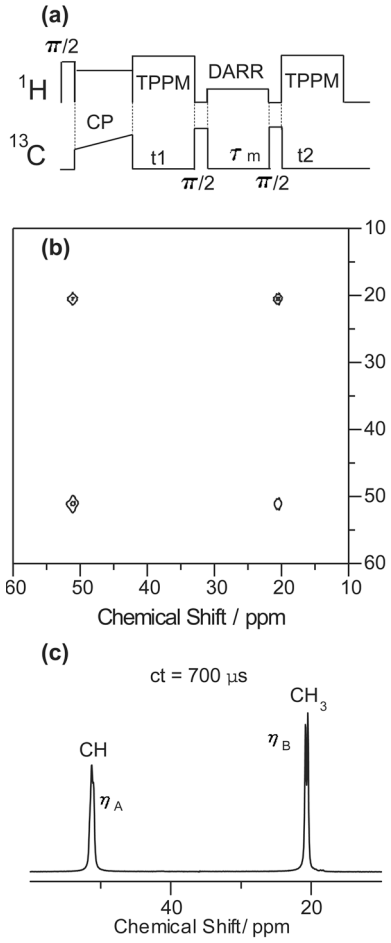

FIG. 3. (a) Pulse sequence for $^{13}C-^{13}C$ 2D exchange NMR using DARR recoupling during the mixing time τ_m. (b) The $^{13}C-^{13}C$ 2D exchange NMR spectrum of [2,3-^{13}C] *l*-alanine taken with DARR at $\tau_m=10$ ms and the CP contact time of 700 μs. (c) The 1D ^{13}C spectrum taken at the CP contact time of 700 μs used to estimate the CP enhancement factors. Each signal becomes doublet due to the $^{13}C-^{13}C$ *J* coupling.

$$K = k/2, \tag{3}$$

where k represents the exchange rate of the polarization transfer (A for methine and B for methyl). Note here that we consider a two-spin system with identical molar fractions. The diagonal elements in $\mathbf{L}$ include the spin-lattice relaxation rates R_{1l} ($l=A$ or B) and the exchange rate as

$$R_{ll} = R_{1l} + K. \tag{4}$$

By using $\mathbf{L}$, the mixing-time (τ_m) dependence of magnetizations [$M_A(\tau_m)$ and $M_B(\tau_m)$] is described as the following simultaneous differential equations:

$$\frac{d}{d\tau_m}\begin{pmatrix} M_A(\tau_m) \\ M_B(\tau_m) \end{pmatrix} = \mathbf{L}\begin{pmatrix} M_A(\tau_m) \\ M_B(\tau_m) \end{pmatrix}. \tag{5}$$

Following the work of Jeener *et al.*,[15] the intensities of the two diagonal peaks are given by

$$a_{AA}(\tau_m) = M_{0,A}e^{-\sigma\tau_m}\left[\cosh(D\tau_m) - \frac{\delta}{D}\sinh(D\tau_m)\right], \tag{6}$$

and

$$a_{BB}(\tau_m) = M_{0,B}e^{-\sigma\tau_m}\left[\cosh(D\tau_m) + \frac{\delta}{D}\sinh(D\tau_m)\right], \tag{7}$$

and those of the two cross peaks are

$$a_{BA}(\tau_m) = M_{0,B}\frac{K}{D}e^{-\sigma\tau_m}\sinh(D\tau_m), \tag{8}$$

and

$$a_{AB}(\tau_m) = M_{0,A}\frac{K}{D}e^{-\sigma\tau_m}\sinh(D\tau_m), \tag{9}$$

with

$$D = \sqrt{\delta^2 + K^2}, \tag{10}$$

$$\sigma = K + \frac{R_{1A} + R_{1B}}{2}, \tag{11}$$

and

$$\delta = \frac{R_{1A} - R_{1B}}{2}. \tag{12}$$

Equations (8) and (9) show that the intensities of the two cross peaks become unequal when their initial intensities $M_{0,A}$ and $M_{0,B}$ are unequal. Here, we consider that the unequal initial intensities are brought about as a result of different CP enhancement for A and B:

$$\frac{a_{AB}(\tau_m)}{a_{BA}(\tau_m)} = \frac{M_{0,A}}{M_{0,B}} = \frac{\eta_A}{\eta_B}, \tag{13}$$

where η_l is the CP enhancement factor for spin l.

Figure 3(b) shows the 2D DARR exchange spectrum of 2,3-Ala at the mixing time of $\tau_m=100$ ms, showing apparently asymmetric cross-peak intensities. The spectrum was taken with a CP contact time (CT) of 700 μs. The CP enhancement factors are estimated to be $\eta_A=2.38$ and $\eta_B=2.54$ from the corresponding one-dimensional (1D) CP spectrum [Fig. 3(c)] taken with the same contact time of 700 μs. While Eq. (13) gives similar cross-peak intensities $a_{AB}/a_{BA}\sim 0.94$, the experimental ratio, $a_{AB}/a_{BA}\sim 0.73$, is much smaller, indicating additional causes of asymmetry.

Further, to examine the mixing-time dependence of the peak intensities, we observed 2D exchange spectra at different mixing times ($\tau_m=5, 10, 20, 50, 100$, and 200 ms) with two different CT values (700 and 50 μs). For CT=50 μs, the CP enhancement factors are estimated to be $\eta_A=2.06$ and $\eta_B=0.84$ from the corresponding 1D spectrum (not shown). Figures 4(a)–4(d) show the mixing-time dependence at CT=700 μs [(a) and (b): diagonal-peak intensities, (c) and (d): cross-peak intensities], and Figs. 4(e)–4(h) at CT=50 μs [(e) and (f): diagonal-peak intensities, (g) and (h): cross-peak intensities]. The observed intensities for CT=700 μs are least-squares fit to Eqs. (6)–(9) using K and M_0 as adjustable parameters ($M_0=M_{0,l}/\eta_l$ and $l=A,B$). The spin-lattice relaxation rates R_{1l} necessary for fitting were determined from initial decays of each magnetization (not shown) observed by using Torchia's sequence,[18] and were found to be $R_{1A}=0.19$ Hz and $R_{1B}=12$ Hz. The dotted lines in Fig. 4 are the best-fit curves with the best-fit exchange rate $k=30$ Hz. The

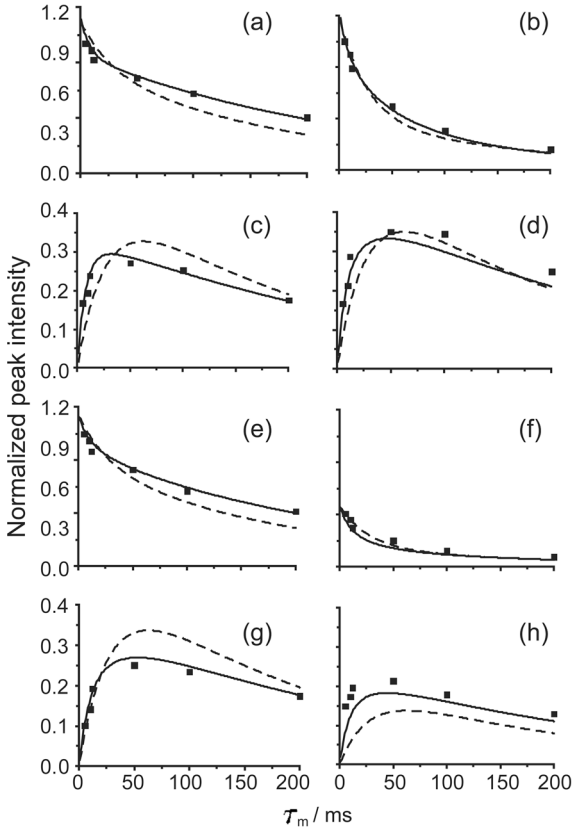

FIG. 4. Mixing-time (τ_m) dependences of peak intensities of a_{AA} [(a) and (e)], a_{BB} [(b) and (f)], a_{AB} [(c) and (g)], and a_{BA} [(d) and (h)]. Dotted and solid lines are the best-fit curves with Eqs. (6)–(9) and (17), respectively. Squares represent experimental data. (a)–(d) were taken at a CP contact time of 700 μs and (e)–(h) at 50 μs. Each peak intensity is given by taking the largest peak intensity at corresponding contact time, a_{BB} (τ_m=5 ms) at CT =700 μs or a_{AA} (τ_m=5 ms) at CT=50 μs, as 1.0.

observed intensities at CT=50 μs are fitted to Eqs. (6)–(9) using M_0 as an adjustable parameter with k=30 Hz. In Fig. 4, the dotted lines apparently deviate from the experimental data (squares), confirming further that the different CP enhancement cannot fully explain the observed asymmetry.

Further, we plot the observed ratios a_{AB}/a_{BA} in Fig. 5 for CT=700 μs (a) and CT=50 μs (b) with the calculated lines using Eq. (13). Although Eq. (13) predicts the constant ratios for the mixing time (dotted lines), the observed ratios from the experimental data (squares) apparently depend on the mixing time τ_m. It indicates that the simple two-site model [Eq. (5)] is inconsistent with the experiments. To explain the observed mixing-time dependence of the ratio of the cross-peak intensities, we modify the two-site model in the following section.

B. The four-site model

Here, we separate each l magnetization (l=A or B) into two groups: $M_{l1}(\tau_m)$ is the magnetization involved in the transfer and $M_{l2}(\tau_m)$ is the magnetization not involved in the transfer (Fig. 6). We assume that M_{l1} and M_{l2} can exchange magnetizations with a rate k_l (the intraspin exchange rate), and the ratio of the initial magnetizations is given by

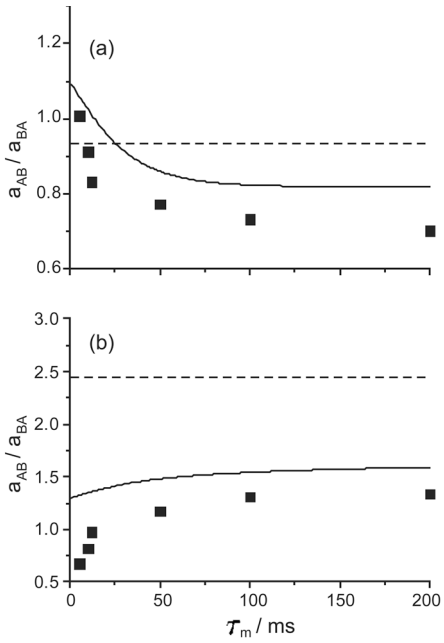

FIG. 5. Mixing-time (τ_m) dependences of the ratio of the cross peaks, a_{AB}/a_{BA}, at CT=700 μs (a) and CT=50 μs (b). Dotted lines are the calculated ones using the values of Eq. (13), and solid lines are those using Eq. (17) with the best-fit parameters. Squares represent the experimental data.

$$M_{l1}(\tau_m=0):M_{l2}(\tau_m=0)=\lambda_l:1-\lambda_l. \tag{14}$$

The exchange is therefore represented by using the following differential equations:

$$\frac{d}{d\tau_m}\begin{pmatrix} M_{A1}(\tau_m) \\ M_{A2}(\tau_m) \\ M_{B1}(\tau_m) \\ M_{B2}(\tau_m) \end{pmatrix} = \mathbf{L}\begin{pmatrix} M_{A1}(\tau_m) \\ M_{A2}(\tau_m) \\ M_{B1}(\tau_m) \\ M_{B2}(\tau_m) \end{pmatrix}. \tag{15}$$

The exchange matrix $\mathbf{L}$ in Eq. (15) includes the intraspin exchange rate k_l for the l spin (l=A or B) and the exchange rate (k=$2K$) between A and B as

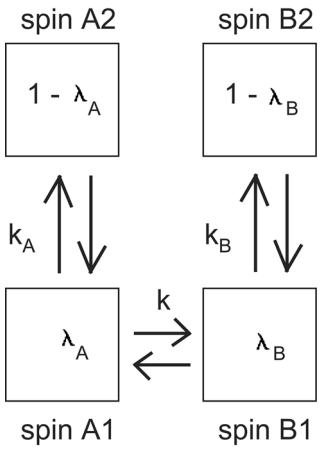

FIG. 6. Schematic model to express the magnetization exchange process of a two-spin (A and B) system under DARR recoupling. The magnetization of each spin is divided into two groups as represented by boxes, one that can exchange polarization as indicated by arrows. The relative ratios given by $\lambda_l(l=A,B)$ are assumed to be constant during the transfer.

$$\mathbf{L}=\begin{pmatrix} -R_{1A}-k_A/2-K & k_A/2 & K & 0 \\ k_A/2 & -R_{1A}-k_A/2 & 0 & 0 \\ K & 0 & -R_{1B}-k_B/2-K & k_B/2 \\ 0 & 0 & k_B/2 & -R_{1B}-k_B/2 \end{pmatrix}. \tag{16}$$

A solution of Eq. (15) is formally written as

$$\begin{pmatrix} M_{A1}(\tau_m) \\ M_{A2}(\tau_m) \\ M_{B1}(\tau_m) \\ M_{B2}(\tau_m) \end{pmatrix} = \exp(\mathbf{L}\tau_m) \begin{pmatrix} \lambda_A M_A(\tau_m=0) \\ (1-\lambda_A)M_A(\tau_m=0) \\ \lambda_B M_B(\tau_m=0) \\ (1-\lambda_B)M_B(\tau_m=0) \end{pmatrix}, \tag{17}$$

which is solved numerically to calculate the cross- and diagonal-peak intensities at τ_m.

By using this four-site model [Eq. (17)] with λ_A, λ_B, K, k_A, k_B, and M_0 as adjustable parameters, we achieved better fitting to the observed mixing-time dependences of the signal intensities of the diagonal and the cross peaks at CT $=700$ μs [solid lines in Figs. 4(a)–4(d)]. Other parameters of R_{1A}, R_{1B}, η_A, and η_B were those determined separately as described above. The best-fit exchange rate $k=106$ Hz and the best-fit intraspin exchange rates $k_A=56$ Hz and $k_B=2.6$ Hz were obtained. The observed intensities at CT $=50$ μs were fitted to Eq. (17) with λ_A, λ_B, and M_0 as adjustable parameters with the best-fit k, k_A, and k_B at CT $=700$ μs. The solid lines in Fig. 4 are the best-fit ones with the parameters $\lambda_A=0.67$ and $\lambda_B=0.57$ for CT$=700$ μs, and $\lambda_A=0.45$ and $\lambda_B=0.84$ for CT$=50$ μs.

The solid lines in Fig. 5 are the ratios a_{AB}/a_{BA} calculated with the best-fit parameters, and are qualitatively consistent with the experimental data. The apparent deviation is ascribed to errors associated with the small cross-peak intensities.

In the above, it was shown that the four-site model (Fig. 6) can explain the observed mixing-time dependence of the diagonal and cross peaks. Hence, each spin is separated into two groups, one is involved in transfer and the other is not involved, and there is an exchange between them. We ascribe this separation to the partial spectral overlap that occurs in the case of the ^{1}H-driven recoupling (Ref. 4) and ^{13}C–^{1}H dipolar-driven recoupling such as DARR.[10] In such recoupling, the ^{13}C–^{1}H dipolar interaction is introduced during the mixing time by either simply turning off ^{1}H decoupling for the former or applying a ^{13}C–^{1}H recoupling method for the latter. The ^{13}C line broadening due to ^{13}C–^{1}H dipolar couplings realizes spectral overlap for a pair of ^{13}C spins with different chemical shifts necessary for energy conservation in ^{13}C–^{13}C polarization transfer. In other words, ^{13}C–^{13}C polarization transfer occurs only for a pair of ^{13}C spins with a particular internuclear orientation to have common resonance frequencies.

C. Effects of partial spectral overlap under DARR and ^{1}H flip-flop motion

To appreciate the spectral overlap under DARR, we observed ^{13}C–^{1}H recoupled signals of the methyl and the methine carbons of 2,3-Ala separately [Figs. 7(b) and 7(c)] by using the sequence in Fig. 7(a). For a ^{13}C–^{1}H spin system under DARR recoupling, the ^{13}C signal becomes a doublet with the recoupled ^{13}C–^{1}H interaction. One such example is the spectrum of the methine carbon shown in Fig. 7(b). In this spectrum, a symmetric lineshape is observed as a result of powder summation of ^{13}C–^{1}H doublet peaks. One of the doublet is a ^{13}C transition associated with the ^{1}H spin state of $|+\frac{1}{2}\rangle$ and the other with $|^1\mathrm{H}\rangle=|-\frac{1}{2}\rangle$. In Fig. 7(b), we

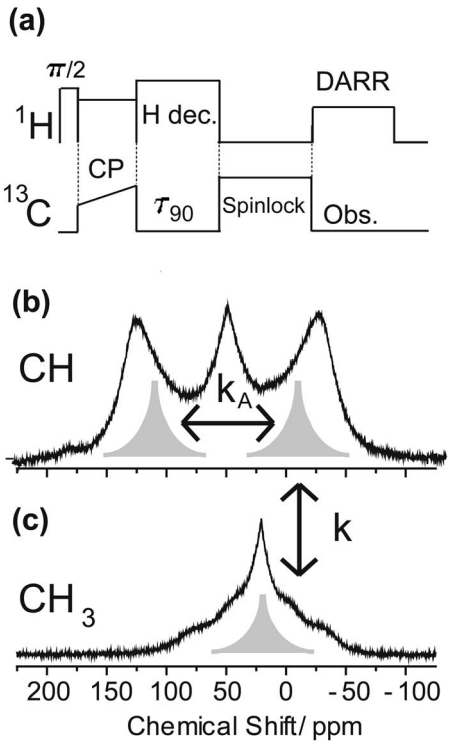

FIG. 7. (a) Pulse sequence for selective observation of one of the two ^{13}C signals of methine and methyl in 2,3-Ala under DARR. The spectrometer transmitter frequency and the evolution time τ_{90} are set so that the two magnetizations line up along the orthogonal axes at the end of τ_{90} (Ref. 24). The following ^{13}C rf irradiation spin locks one of the magnetizations, while the other magnetization decays rapidly due to $T_{2\rho}$. The spin-locked magnetization is then observed under DARR to appreciate the ^{13}C–^{1}H recoupled ^{13}C spectrum: (b) the methine carbon and (c) the methyl carbon. In the present experiment, the spin-lock time of 5 ms was enough to reduce the unlocked magnetization. In (b) and (c), shaded peaks schematically illustrate a doublet and singlet of a methine and a methyl carbon of a pair, respectively. The arrows among them indicate polarization transfer with the intraspin exchange rate k_A and the exchange rate k.

schematically draw a $^{13}C-^{1}H$ doublet of the methine carbon together with the observed spectrum for explanation. Further, we assume that the corresponding methyl signal of the pair is a singlet peak as illustrated in Fig. 7(c). In this particular case, one of the doublet peaks of the methine carbon has spectral overlap with the methyl singlet peak, while the other peak in the doublet does not. However, the ^{1}H flip-flop transition caused by the $^{1}H-^{1}H$ dipolar interactions would exchange the positions of the ^{13}C signals of the methine doublet.[19] The whole exchange process for this pair can then be expressed by using the following equation:

$$\frac{d}{d\tau_m}\begin{pmatrix} M_{A1} \\ M_{A2} \\ M_{B1} \end{pmatrix} = \begin{pmatrix} -R_{1A}-k_A/2-K & k_A/2 & K \\ k_A/2 & -R_{1A}-k_A/2 & 0 \\ K & 0 & -R_{1B}-K \end{pmatrix}\begin{pmatrix} M_{A1} \\ M_{A2} \\ M_{B1} \end{pmatrix}, \tag{18}$$

with the initial magnetizations as $M_{A1}(\tau_m=0):M_{A2}(\tau_m=0):M_{B1}(\tau_m=0)=0.5:0.5:1$. Note here that we assumed a singlet methyl peak, i.e., $M_{B2}(\tau_m)=0$. On the other hand, for a pair with a smaller splitting for the methine doublet, both of the doublet peaks can participate in the transfer and the corresponding equation becomes

$$\frac{d}{d\tau_m}\begin{pmatrix} M_{A1} \\ M_{B1} \end{pmatrix} = \begin{pmatrix} -R_{1A}-K & K \\ K & -R_{1B}-K \end{pmatrix}\begin{pmatrix} M_{A1} \\ M_{B1} \end{pmatrix}, \tag{19}$$

with the initial magnetizations as $M_{A1}(\tau_m=0):M_{B1}(\tau_m=0)=1:1$. The phenomenologically deduced 4×4 equation [Eq. (15)] is thus a result of a weighted sum of exchange equations, such as Eqs. (18) and (19), for all pairs in a powdered sample. For example, a simple sum of Eqs. (18) and (19) results in the initial magnetizations of $M_{A1}(\tau_m=0):M_{A2}(\tau_m=0):M_{B1}(\tau_m=0):M_{B2}(\tau_m=0)=0.75:0.25:1:0$, which leads to unequal initial magnetizations. Orientational dependence of the CP enhancement[20] can also affect the unequal initial magnetizations. At a short contact time, ^{13}C magnetizations with the stronger $^{13}C-^{1}H$ dipolar couplings are enhanced more than those with the weaker $^{13}C-^{1}H$ couplings, leading to the different ratios of the initial magnetizations for the different CT values.

In this work, we attributed the intraspin exchange to ^{1}H flip-flop dynamics. However, the obtained intraspin exchange rates $k_A=70$ Hz and $k_B=1.4$ Hz are much slower than the ^{1}H dipolar fluctuation rate (~30 kHz) in *l*-alanine obtained from the spin-lattice relaxation study.[21] The diffusion rate at $\nu_R=20$ kHz in the present work is not directly comparable to the ^{1}H dipolar fluctuation rate observed without ^{1}H irradiation at $\nu_R=4.5$ kHz, however, the observed slow rates deserve an explanatory comment. To appreciate effects of MAS on $^{1}H-^{1}H$ dipolar couplings, the ^{1}H spectrum of 2, 3-Ala was observed at a MAS frequency of 20 kHz (Fig. 8). The observed ^{1}H spectrum shows two distinct peaks at ~0 ppm for the methyl protons and at ~9 ppm for NH_3. The peak of the methine proton is also discernible at ~4 ppm. The observed good ^{1}H resolution (linewidth is ~400 Hz) indicates extensive suppression of ^{1}H flip-flop transition as a result of fast MAS ($\nu_R=20$ kHz). Furthermore, fast internal rotation of both the methyl group and the NH_3 group would assist suppression of the $^{1}H-^{1}H$ transition efficiently. The suppression can also be recognized in Figs. 7(b) and 7(c) because fast ^{1}H flip-flop transition would bring broad and characterless lineshapes.

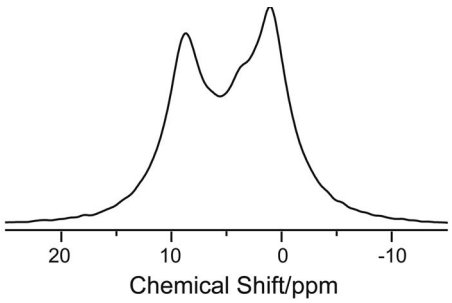

FIG. 8. ^{1}H spectrum of [2,3-^{13}C] *l*-alanine at the MAS frequency of 20 kHz obtained by a single $\pi/2$ pulse.

Since a recoupled $^{13}C-^{13}C$ dipolar coupling has orientational dependence, the obtained rate is an averaged one at best, and it is difficult to derive internuclear distances from *k*. Nevertheless, we found a good correlation among *k* and distances (Refs. 10 and 23), and thus quantitative analysis of the exchange rates is necessary for structural analysis using DARR. This work shows that the four-site model is applicable to the analysis of peak intensities in 2D DARR-exchange NMR. The application is, however, difficult for a larger spin system because of severe signal overlapping for diagonal peaks and also because of the involvement of many spins in the transfer process. Hence, in the following, we examine a much simpler analysis of an initial region of the mixing-time dependence using only the cross-peak intensities and compare with the results using the four-site model.

D. Examination of initial buildup

Here, we assume that the intraspin exchange between spins *l*1 and *l*2 is negligible for a short mixing time ($\tau_m \leqslant 50$ ms). Then, the problem becomes a two-site exchange and Eqs. (6)–(9) can be used with slight modifications. Equations (8) and (9) may be rewritten as

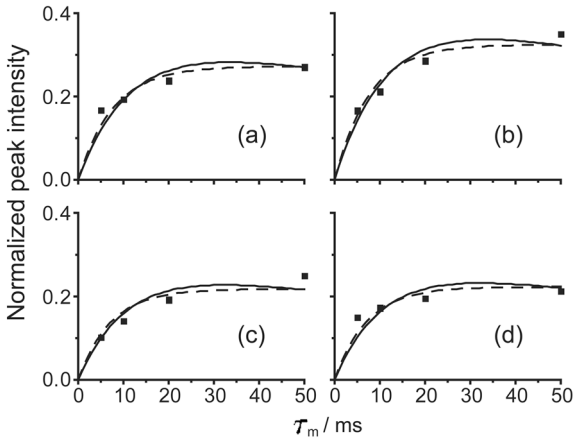

FIG. 9. Mixing-time (τ_m) dependences of the cross-peak intensities ($\tau_m \leqslant 50$ ms) at CT=700 μs [(a) and (b)] and those at CT=50 μs [(c) and (d)]. (a) and (c) are the cross peaks $a_{AB}(\tau_m)$, and (b) and (d) are the cross peaks $a_{BA}(\tau_m)$. Solid lines represent the best-fit curves to Eq. (20) [(a) and (c)] and to Eq. (21) [(b) and (d)]. Dotted lines represent the curves best-fit to Eq. (22) [(a) and (c)] and to Eq. (23) [(b) and (d)].

$$a_{AB}(\tau_m) \sim a_{AB}^0 \frac{k}{D} e^{-\sigma\tau_m} \sinh(D\tau_m) \tag{20}$$

and

$$a_{BA}(\tau_m) \sim a_{BA}^0 \frac{k}{D} e^{-\sigma\tau_m} \sinh(D\tau_m), \tag{21}$$

and the observed cross-peak intensities for $\tau_m \leqslant 50$ ms were fitted to Eqs. (20) and (21) by taking a_{AB}^0, a_{BA}^0, and k as adjustable parameters. Again R_{1A} and R_{1B}, determined separately, were used in the fitting. Solid lines in Fig. 9 represent the best-fit curves with the best-fit values of $k=80$ Hz at CT=700 μs and $k=85$ Hz at CT=50 μs. The best-fit k values (80–85 Hz) are much larger than the best-fit k of 30 Hz obtained by using the data up to $\tau_m=200$ ms (Fig. 4) and are closer to the best-fit k value (106 Hz) obtained by using the four-site model. This indicates that the two-site model is not applicable for the longer τ_m region, where the effects of the intraspin diffusion become appreciable.

By further assuming $k \gg R_{1A}$ and R_{1B}, we have

$$a_{AB}(\tau_m) \sim a_{AB}^0[1-\exp(-k\tau_m)] \tag{22}$$

and

$$a_{BA}(\tau_m) \sim a_{BA}^0[1-\exp(-k\tau_m)]. \tag{23}$$

It is also possible to fit the data to Eqs. (22) and (23) (dotted lines in Fig. 9), and we obtained $k=129$ Hz at CT=700 μs and $k=140$ Hz at CT=50 μs. The obtained k values using Eqs. (20) and (21) (80–85 Hz) and using Eqs. (22) and (23) (129–140 Hz) deviate significantly from $k=106$ Hz obtained by using the four-site model. Therefore, the analysis of 2D DARR exchange NMR data using the initial-rat e assumptions with the two-sites model should be carefully done.

IV. CONCLUDING REMARKS

The DARR recoupling examined in this work corresponds to that classified as the second-order DARR in Ref. 10, because the chemical-shift difference of the two spins are smaller than the $^{13}C-^{1}H$ dipolar broadening. For the first-order DARR, which works for a pair of spins whose spectral overlap is achieved between one of the spinning sidebands of one of the pair spin and the center band of the other, we can still apply the present theory; for the spin whose sideband is overlapped with the center band of the other, almost all of its magnetization is involved in transfer, and for the spin whose center band is overlapped with the other's sideband, only a part of magnetization is involved.

The asymmetry found in 2D exchange spectra using other homonuclear recoupling methods, for example, RFDR, C7, etc., can most likely be ascribed to nonuniform CP enhancement. Lastly, we would like to recommend NOP (Refs. 22 and 23) instead of CP for a fully ^{13}C-labeled molecule containing methyl groups, because NOP has two advantages over CP: (i) the signal enhancement is more uniform, and (ii) the enhancement factor is larger.

Note added in proof. It has recently come to the author's attention that the effect of CP has also been examined by S. Caldarelli and L. Emsley, J. Magn. Reson. **130**, 233 (1988).

ACKNOWLEDGMENTS

This research was financially supported in part by CREST, JST, and in part by Special Coordination Funds from Promoting Science and Technology of MEXT.

[1] R. R. Ernst, G. Bodenhausen, and A. Wokaun, *Principles of nuclear magnetic resonance in one and two dimensions* (Clarendon, Oxford, 1987).
[2] For a review, see J. Cavanagh, W. J. Fairbrother, A. G. Palmer III, and N. J. Skelton, *Protein NMR Spectroscopy* (Academic, New York, 1996).
[3] F. Castellani, B. van Rossum, A. Diehi, M. Schubert, K. Rehbein, and H. Oschkinat, Nature (London) **420**, 98 (2002).
[4] For a review, see B. H. Meier, Adv. Magn. Opt. Reson. **18**, 1 (1994).
[5] A. E. Bennett, J. H. Ok, R. G. Griffin, and S. Vega, J. Chem. Phys. **96**, 8624 (1992).
[6] N. C. Nielsen, H. Bildsœ, H. J. Jakobsen, and M. H. Levitt, J. Chem. Phys. **101**, 1805 (1994).
[7] J. M. Joers, R. Rosanske, T. Gullion, and J. R. Garbow, J. Magn. Reson., Ser. A **106**, 123 (1994).
[8] Y. K. Lee, N. D. Kurur, M. Helmle, O. Johannessen, N. C. Nielsen, and M. H. Levitt, Chem. Phys. Lett. **242**, 304 (1995).
[9] K. Takegoshi, S. Nakamura, and T. Terao, Chem. Phys. Lett. **344**, 631 (2001).
[10] K. Takegoshi, S. Nakamura, and T. Terao, J. Chem. Phys. **118**, 2325 (2003).
[11] W. T. Franks, D. H. Zhou, B. J. Wylie, B. G. Money, D. T. Graesser, H. L. Frericks, G. Sahota, and C. M. Rienstra, J. Am. Chem. Soc. **127**, 12291 (2005).
[12] T. I. Igumenova, A. E. McDermott, K. W. Zilm, R. W. Martin, E. K. Paulson, and A. J. Wand, J. Am. Chem. Soc. **126**, 6720 (2004).
[13] E. Crocker, A. B. Patel, M. Eilers, S. Jayaraman, E. Getmanova, P. J. Reeves, M. Ziliox, H. G. Khorana, M. Sheves, and S. O. Smith, J. Biomol. NMR **29**, 11 (2004).
[14] Y. Masuda, K. Irie, K. Murakami, H. Ohigashi, R. Ohashi, K. Takegoshi, T. Shimizu, and T. Shirasawa, Bioorg. Med. Chem. **13**, 6803 (2005).
[15] J. Jeener, B. H. Meier, P. Bachmann, and R. R. Ernst, J. Chem. Phys. **71**, 4546 (1979).
[16] S. K. Brahmachari, T. N. Bhat, V. Sudhakar, M. Vijayan, R. S. Rapaka, R. S. Bhatnagar, and V. S. Ananthanarayanan, J. Am. Chem. Soc. **103**, 1703 (1981).
[17] A. E. Bennett, C. M. Rienstra, M. Auger, K. Lakshmi, and R. G. Griffin, J. Chem. Phys. **103**, 6951 (1995).
[18] D. A. Torchia, J. Magn. Reson. (1969-1992) **30**, 613 (1978).
[19] K. Takegoshi and C. A. McDowell, J. Chem. Phys. **86**, 6077 (1987).

[20] A. Pines, M. G. Gibby, and J. S. Waugh, J. Chem. Phys. **59**, 569 (1973).
[21] K. Akasaka, S. Ganapathy, C. A. McDowell, and A. Naito, J. Chem. Phys. **78**, 3567 (1983).
[22] K. Takegoshi and T. Terao, J. Chem. Phys. **117**, 1700 (2002).
[23] E. Katoh, K. Takegoshi, and T. Terao, J. Am. Chem. Soc. **126**, 3653 (2004).
[24] C. Connor, A. Naito, K. Takegoshi, and C. A. McDowell, Chem. Phys. Lett. **113**, 123 (1985).